Conceptual Design and Performance Analysis for a Large Civil Compound Helicopter

Carl Russell and Wayne Johnson
Aeromechanics Branch
National Aeronautics and Space Administration
Ames Research Center, Moffett Field, California
carl.russell@nasa.gov, wayne.johnson@nasa.gov

Abstract

A conceptual design study of a large civil compound helicopter is presented. The objective is to determine how a compound helicopter performs when compared to both a conventional helicopter and a tiltrotor using a design mission that is shorter than optimal for a tiltrotor and longer than optimal for a helicopter. The designs are generated and analyzed using conceptual design software and are further evaluated with a comprehensive rotorcraft analysis code. Multiple metrics are used to determine the suitability of each design for the given mission. Plots of various trade studies and parameter sweeps as well as comprehensive analysis results are presented. The results suggest that the compound helicopter examined for this study would not be competitive with a tiltrotor or conventional helicopter, but multiple possibilities are identified for improving the performance of the compound helicopter in future research.

NOMENCLATURE

Acronyms

CAMRAD II	Comprehensive Analytical Model of Rotorcraft Aerodynamics and Dynamics
ISA	International Standard Atmosphere
LCTR	Large Civil TiltRotor
NDARC	NASA Design and Analysis of Rotorcraft
OGE	Out of Ground Effect
OEI	One Engine Inoperative
V/STOL	Vertical/Short Take-Off and Landing

Symbols

AR	Wing aspect ratio
C_T	Rotor thrust coefficient
C_W	Weight coefficient
C_{Po}	Rotor profile power coefficient
C_{Do}	Wing parasite drag coefficient
$c_{d\ mean}$	Rotor mean blade drag coefficient
D_{eff}	Effective drag
D_{wing}	Wing drag
D_{rotor}	Main rotor drag
e	Wing span efficiency
K	1,000 ft altitude
L_{wing}	Wing lift
L/D_{eff}	Effective lift-to-drag ratio
P	Power required
P_i	Induced power
P_o	Profile power
P_p	Parasite power
P_{rotor}	Main rotor power
q	Dynamic pressure
S	Wing planform area
V	Forward velocity
V_{br}	Velocity for maximum range
V_{be}	Velocity for maximum endurance
X	Wind axis drag force
η_{prop}	Propulsive efficiency
κ	Induced power factor
μ	Edgewise advance ratio
μ_z	Axial advance ratio
σ	Rotor solidity (thrust weighted)

Presented at the AHS Future Vertical Lift Aircraft Design Conference, San Francisco, CA, January 18-20, 2012.

INTRODUCTION

With passenger airline delays reaching all-time highs due to increasing airport congestion, vertical and short takeoff and landing (V/STOL) aircraft are uniquely equipped to increase airport throughput without significant runway improvements or expansion.[1,2] To fill this need, conventional helicopters are well suited to short trips on the order of 100 nm. Previous research has shown that tiltrotors are well suited for longer trips on the order of 1,000 nm.[3] The focus of this study is to determine whether a third configuration – a slowed-rotor compound helicopter – can be a better choice than either a conventional helicopter or a tiltrotor for an intermediate distance of 500 nm.

To assess the competitiveness of the compound helicopter, three designs were created: a conventional helicopter, a compound, and a tiltrotor. Each is capable of carrying a payload of 90 passengers, or 19,800 lb. All three designs use the same fuselage geometry so that passenger accommodation is consistent, and they use the same engine performance model. Aside from the fuselage, payload, and engine specifications, the three aircraft designs are independent.

This study is not intended to design any prototype aircraft, but rather to suggest designs that are best capable of meeting given mission constraints. These designs will necessarily

contain assumptions about future technology improvements in both aircraft and infrastructure. The impact of these assumptions is outside the scope of this study, but will be addressed by future research.

BACKGROUND

In a conventional helicopter, forward speed is limited by retreating blade stall, which can severely limit lift and propulsive thrust at high speeds. There are multiple methods of compounding a helicopter to achieve higher flight speeds. With lift compounding, a wing is added to the aircraft to unload the main rotor. Thrust compounding adds a propulsor, such as a propeller or jet engine to provide the necessary thrust for high speeds. Compressibility drag on the advancing side of the main rotor limits forward speed as well, so as the advancing tip Mach number approaches or exceeds 1, the rotational speed of the rotor must be reduced. The compound helicopter design presented in this paper uses a slowed-rotor, and is fully compounded, with both a wing and auxiliary propulsion.

Compound helicopters have never been mass-produced for civilian passenger transportation, but various prototypes have been built for both military and civil applications. A notable example of a military compound is the Lockheed AH-56 Cheyenne, which was a fully compounded helicopter using a pusher propeller and a low-mounted wing.[4] The Cheyenne was developed in the late 1960s for the US Army as an attack helicopter, but the program was canceled after only 10 had been built. With a top speed of 212 kt, the Cheyenne could reach higher speeds than its conventional helicopter counterparts. A recently developed experimental compound helicopter is the Eurocopter X3, which slows the main rotor in cruise and uses two tractor propellers mounted on short wings for additional propulsion in cruise and anti-torque in hover.[5] Using compound helicopter technology, the X3 has been able to reach speeds over 230 kt.[6]

This study is focused on the design of a rotorcraft with a payload of approximately 20,000 lb. While no compound helicopter of this size has been mass-produced, there are prominent examples of conventional helicopters and tiltrotors in this size range. The Bell-Boeing V-22 Osprey is a tiltrotor with a payload of 20,000 lb (but cannot take off vertically with this load).[7] Both the Mil Mi 26 and Sikorsky CH-53E Super Stallion are conventional helicopters with payloads over 30,000 lb.[8,9] None of these rotorcraft is a passenger transport, but they provide good bases for comparison.

A previous NASA study detailed in Ref. 3 focused on designing a heavy lift passenger transport capable of carrying 120 passengers at a cruise speed of 350 kt at 30,000 ft altitude with a range of 1,200 nm. This study examined three configurations: a tiltrotor, a tandem compound, and an "advancing blade concept." In this case, the tiltrotor provided the best characteristics for the design mission; however, the study only looked at a single design mission distance, so it is possible that a compound design would perform better given different mission constraints. This study produced the Large Civil Tiltrotor (LCTR) design, which was followed by a refined version, the LCTR2, designed to carry 90 passengers 1,000 nm at 300 kt and 28,000 ft altitude.[10]

Another study focused on a compound helicopter design weighing 100,000 lb, cruising at 250 kt and 4,000 ft altitude.[11] This study ran sweeps of disk loading, blade loading, and wing loading to determine the effects of these parameters on aircraft performance. More recent conceptual design studies have used both conceptual design and comprehensive analysis software packages to design slowed-rotor compound helicopters in the 30,000 to 40,000 lb range.[12,13,14] The examples given in this section were referred to throughout this study as checks on the three generated designs.

APPROACH

Computational Methods – Sizing

All of the sizing and design tasks were carried out using NASA's rotorcraft design code NDARC. NDARC is a conceptual/preliminary design and analysis code for rapidly sizing and conducting performance analysis of new rotorcraft concepts, with frameworks for introducing multiple levels of fidelity.[15,16,17] NDARC has a modular code base, facilitating its extension to new concepts and the implementation of new computational procedures. NDARC version 1.5 was used in this design activity.

A typical NDARC run consists of a sizing task, followed by off-design performance analysis. During the sizing process, point condition and mission performance are calculated and the aircraft is resized both geometrically and mechanically until the convergence criteria are met.

The NDARC rotor performance model represents the rotor power as the sum of induced, profile, and parasite terms: $P=P_i+P_o+P_p$. The parasite power (including climb/descent power for the aircraft) is obtained from the wind axis drag force and forward velocity: $P_p=-XV$. The induced power is calculated from the ideal power and the induced power factor κ: $P_i=\kappa P_{ideal}$. The profile power is calculated from a mean blade drag coefficient: $C_{Po} = (\sigma/8)c_{d\ mean}F_P$, where the function $F_P(\mu,\mu_z)$ accounts for the increase of the blade section velocity with rotor edgewise and axial speed. The induced and profile power cannot be measured separately in a wind tunnel or flight test; only the sum is available from $P_i+P_o=P+XV$ (if the rotor wind-axis drag force X is measured or estimated). Therefore, analysis is used to separate induced and profile power. The steps in the approach are: first correlate performance calculations from a comprehensive analysis with wind tunnel or flight test data; then calculate rotor performance for the full range of expected flight and operating conditions; finally, develop the parameters of the NDARC rotor performance model based on calculated κ and $c_{d\ mean}$.

Computational Methods – Comprehensive Analysis

Performance analyses for rotor optimization were conducted with the comprehensive rotorcraft analysis CAMRAD II.[18] CAMRAD II is an aeromechanics analysis of rotorcraft that incorporates a combination of advanced technologies, including multibody dynamics, nonlinear finite elements, and rotorcraft aerodynamics. The trim task finds the equilibrium solution for a steady state operating condition, and produces the solution for performance, loads, and vibration. The aerodynamic model includes a wake analysis to calculate the rotor non-uniform induced velocities. CAMRAD II has undergone extensive correlation of performance and loads measurements on helicopters.[19-26]

The CAMRAD II aerodynamic model for the rotor blade is based on lifting-line theory, using steady two-dimensional airfoil characteristics and a vortex wake model. The rotor blade modeling problem of lifting-line theory is unsteady, compressible, viscous flow about an infinite aspect-ratio wing, in a uniform flow consisting of the yawed free stream and the wake-induced velocity. This problem is modeled as two-dimensional, steady, compressible, viscous flow (airfoil tables), plus corrections. Corrections are included for swept and yawed flow and spanwise drag. The wake problem of lifting-line theory is an incompressible vortex wake behind the lifting-line, with distorted geometry and rollup. The wake analysis calculates the rotor non-uniform induced velocity using either rigid or free wake geometry. The concentrated tip vortices are the key features of the rotor wake, important for performance, airloads, structural loads, vibration, and noise calculations. The formation of the tip vortices is modeled in CAMRAD II, not calculated from first principles.

For this study, rotor performance optimization in CAMRAD II considered a single main rotor for each of the three designs, and the calculations for calibration of the sizing code rotor models consider an isolated rotor. Rotor performance was calculated using non-uniform inflow with rigid wake geometry in high speed cruise and free wake geometry in hover. Airfoil characteristics were obtained from tables representing advanced technology airfoils.

For calibration of the sizing code performance model, various sweeps were performed in both cruise and hover conditions. In hover, C_T/σ was swept through the range of expected thrust conditions. In cruise, forward and vertical thrust, along with forward velocity were varied through the expected envelope of operations for each of the three rotorcraft designs.

Design Process

Airlines or other operators will likely be primarily concerned with both airframe purchase price and operational costs. For this study, empty weight, engine power, and fuel burn were used in lieu of cost. Initial purchase price of aircraft tends to correlate well with empty weight, so the airframes here are designed for minimum weight.[27] Increased global crude oil prices in the last several years have driven airline fuel costs up so that they now comprise approximately half of direct operating cost.[28] For this reason, fuel burn is a good indication of the cost to operate a particular design. Engine cost also naturally scales with power, so minimum power designs are desirable.

The iterative design process that was used for this study is illustrated in Fig. 1. Tasks of the design process utilizing NDARC are contained in the heavier square boxes, while tasks that used CAMRAD II are contained in the lighter rounded boxes.

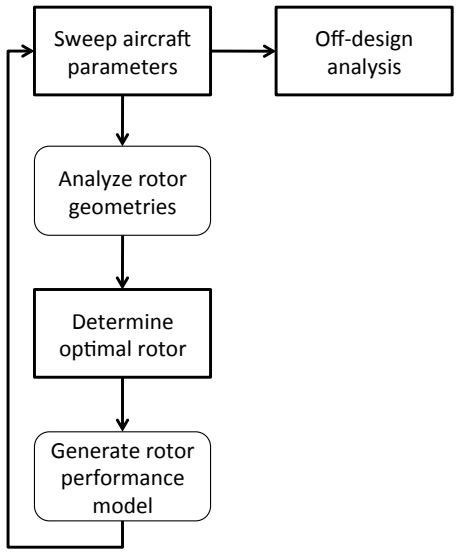

Figure 1. Iterative design process

The process for each of the three aircraft was substantially the same, and the steps are outlined below. More thorough descriptions of the process for each of the three designs are presented later.

1. Sweep aircraft parameters
   Aircraft characteristics such as wing loading, disk loading, and number of rotor blades are varied in NDARC using a generic rotor model, resulting in a baseline configuration.

2. Analyze rotor geometries
   Rotor geometry is varied and simulated in CAMRAD II at the design flight conditions to develop a set of candidate rotors.

3. Determine optimal rotor
   Performance characteristics of the candidate rotor designs are used in NDARC to determine the best rotor for the design mission.

4. Generate rotor performance model
   Using the optimal rotor geometry, simulate various flight conditions in CAMRAD II to generate a math model of the rotor power consumption.

5. Sweep aircraft parameters 2
   With the rotor performance model determined, sweep aircraft characteristics again to arrive at a revised optimal configuration. If necessary, steps 2-4 can be repeated as many times as desired. For this study, the loop was only completed once for each aircraft.

6. Off-design analysis
   Once the aircraft configuration is determined, NDARC can be used to analyze different operating conditions and missions.

AIRCRAFT DESIGNS

Three aircraft were designed for this study: a compound helicopter, a tiltrotor, and a conventional helicopter. All three designs have identical fuselage, payload, and crew specifications. The mission length is the same for all three aircraft, but the required minimum speeds for each are different, reflecting the expected cruise speeds of each configuration. Cruise altitude for the compound and conventional helicopter were chosen based on preliminary parametric sweeps, but was not rigorously optimized. For the tiltrotor, cruise altitude was the same as in Ref. 10. Technology levels assumed for the three aircraft are consistent with those used in Ref. 3. The baseline design mission and required performance conditions for the three aircraft are summarized in Table 1. An overview of each of the designs is presented here along with the final results of the sizing process, which are summarized in Table 2. The details of the design process are contained in a later section.

Table 1. Design mission for all three designs

Design Mission
3 min taxi, 5K ISA +25˚C
2 min hover OGE 5K ISA +25˚C
Climb at minimum *P* margin (credit distance to cruise segment)
Cruise at V_{br} for 500 nm range at given altitude
Compound: 20K ISA
Tiltrotor: 28K ISA
Helicopter: 12K ISA
Descend at V_{br} (no range credit)
1 min hover OGE, 5K ISA +25˚C
Reserve (alternate airport): 100 nm V_{br} at cruise altitude
Reserve (hover): 30 min V_{br} 5k ISA
Performance Requirements
One engine inoperative hover at 5k ISA +25˚C
Minimum cruise speed
Compound: 220 kt at 20K ISA
Tiltrotor: 300 kt at 28K ISA
Helicopter: 150 kt at 12K ISA

Table 2. Design summary for compound helicopter, tiltrotor, and helicopter

	Compound	Tiltrotor	Helicopter
Payload (90 pax), lb	19,800	19,800	19,800
Overall length, ft	127.9	108.9	128.8
Overall width, ft	106.7	141.9	49.0
Max takeoff weight, lb	115,665	97,449	86,617
Empty weight, lb	64,789	55,380	42,060
Mission fuel, lb	14,545	8,098	11,999
Engine max rated power, hp	4×6,996	4×5,150	4×4,020
Main rotor disk loading, lb/ft^2	15.0	15.0	10.0
Main rotor solidity	0.123	0.123	0.137
Main rotor design C_W/σ	0.151	0.151	0.090
Main rotor radius, ft	46.2	32.5	49.0
Main rotor V_{tip}, hover, ft/s	650	650	650
Main rotor V_{tip}, cruise, ft/s	450	400	650
Main rotor number of blades	7	4	7
Wing lift share in cruise	84.2%	100%	—
Wing span, ft	106.7	107.0	—
Wing loading, lb/ft^2	90.0	105.0	—

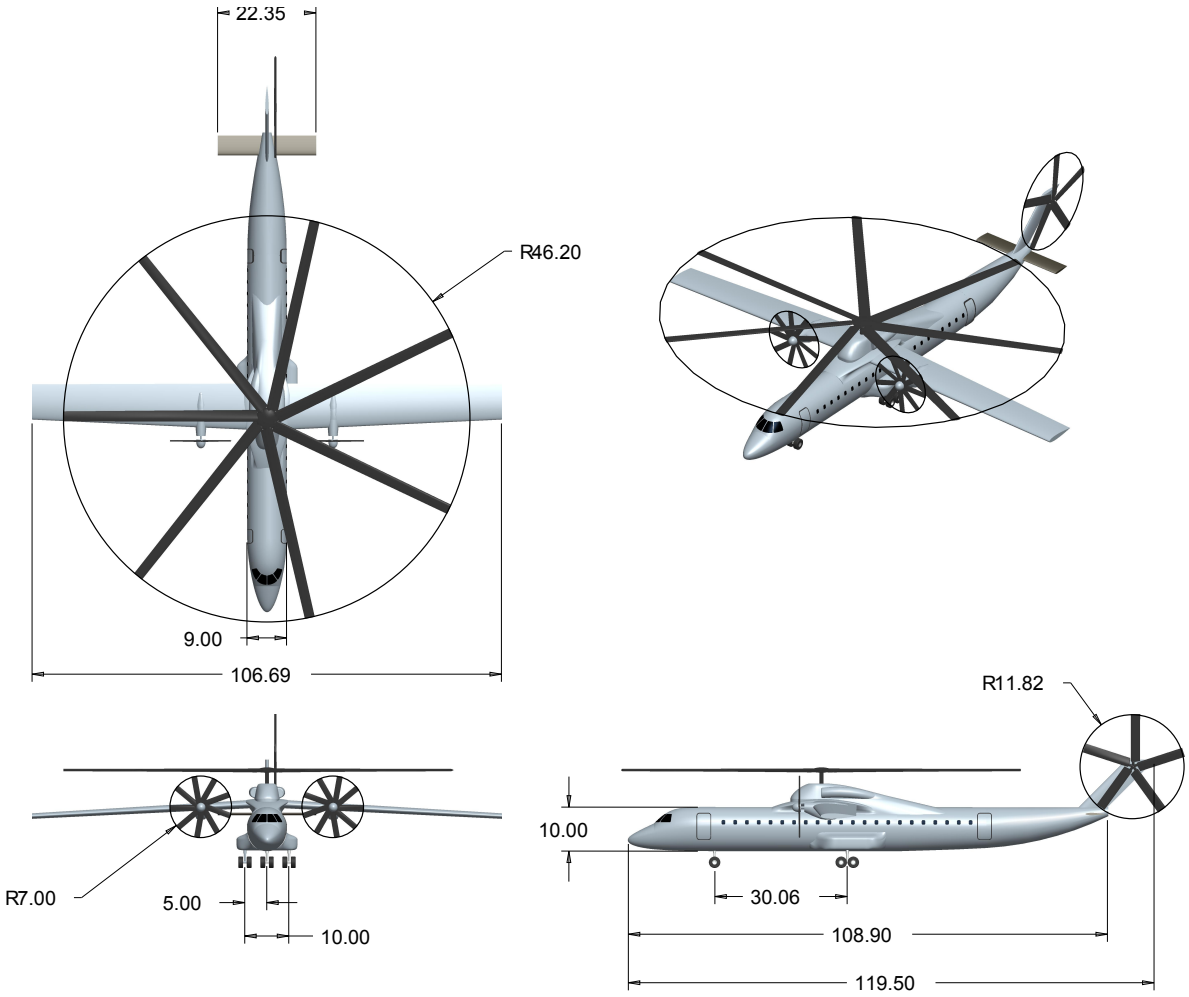

Figure 2. Illustration of the compound helicopter design

Compound Helicopter Design

The compound helicopter design uses a single main rotor and an anti-torque tail rotor. A high wing is used with a tractor propeller on each wing. Initial designs for this study used a configuration similar to the Cheyenne, with a single main rotor, an anti-torque tail rotor, and a single pusher propeller at the tail. The large size of both the anti-torque rotor and the pusher propeller made it impractical to locate both at the tail due to structural and weight considerations, so the configuration with two tractor propellers was used.

Power comes from four turboshaft engines, with two located at each of the propellers. In hover, power is transferred via drive shafts to a main gearbox above the fuselage, which in turn directs power to the main and tail rotors. In cruise, the majority of the engine power is directed to the propellers, while a much smaller amount goes to the main and tail rotors.

Aircraft control in hover is similar to that of a typical helicopter, using main rotor collective, cyclic, and tail rotor collective inputs. In cruise, control is more typical of a fixed-wing airplane, using ailerons, a rudder, and an elevator. The compound design has both a horizontal and vertical tail for stability. The fraction of the total lift carried by the wing is adjusted by main rotor collective and aircraft pitch. Figure 2 shows the layout of the compound helicopter.

Tiltrotor Design

The tiltrotor design is heavily based on the LCTR2, presented in Refs. 10 and 29. It uses a high wing with two four-bladed rotors at each wingtip. Two turboshaft engines are located directly behind each of the rotors. The wing carries a cross shaft from one engine nacelle to the other so that power can be transferred equally to both rotors in an OEI situation.

The tiltrotor empennage consists of a V-tail. Rotor cyclic and collective are used for control in hover, while control surfaces on the wings and tail are used in cruise. The tiltrotor layout is shown in Fig. 3.

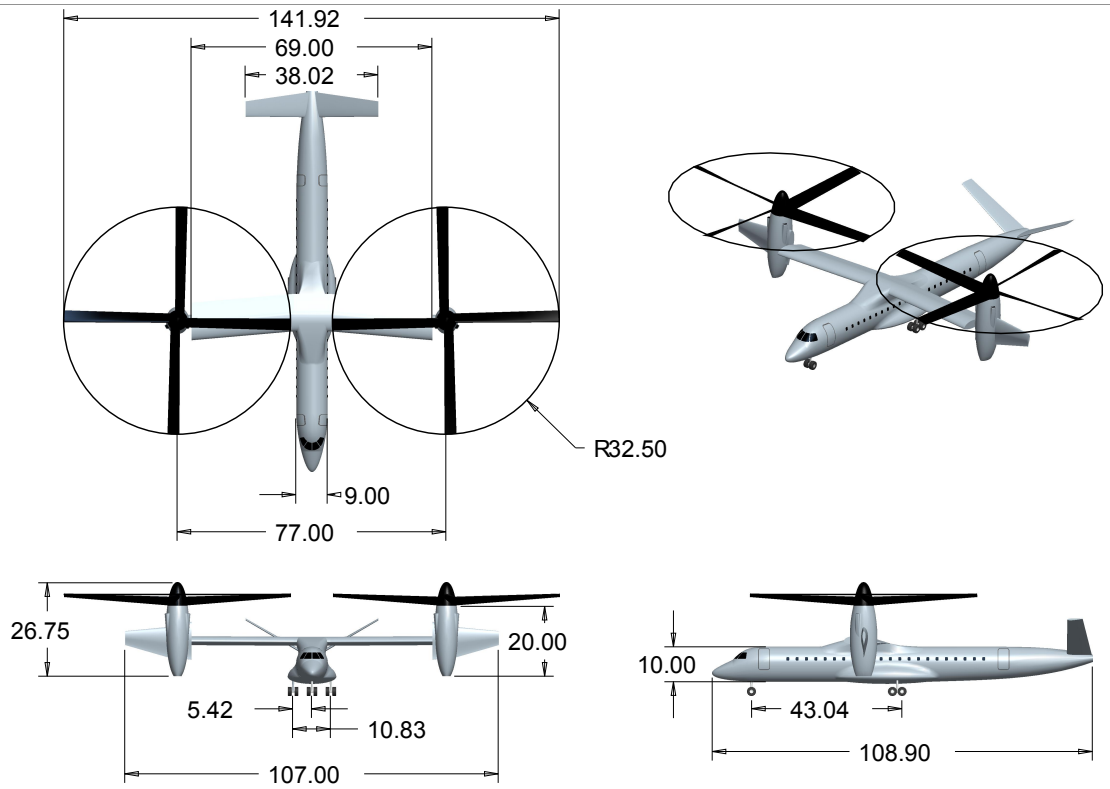

Figure 3. Illustration of the tiltrotor design

Helicopter Design

The conventional helicopter design uses a single main rotor and anti-torque tail rotor. All four engines are located above the fuselage and feed into a main gearbox that distributes power to the main and tail rotors. The control scheme is what would typically be expected of a helicopter for all phases of flight. The layout of the helicopter is shown in Fig. 4.

SIZING

NDARC facilitates the variation of a multitude of rotorcraft design parameters in the sizing process. It does not, however, contain a formal optimization routine, which would allow the simultaneous variation of multiple parameters. Therefore, the selection of design variables must be limited in order to keep the design space from becoming unmanageable. For this study, the primary variables that were changed in the design process were wing loading, disk loading, number of rotor blades, and cruise altitude.

Main and tail rotor hover tip speeds were varied as part of the initial sizing process, and in general, higher hover tip speeds resulted in lighter, more efficient aircraft. The problem with utilizing a higher tip speed is that it results in higher noise levels. Reference 29 used 650 ft/s as the maximum tip speed with acceptable noise characteristics, so this study used this same constraint for all three aircraft.

Designs were compared from a cost standpoint. The combination of empty weight and engine power was used as a proxy for airframe purchase cost. Fuel burn during the design mission was used to represent direct operating cost. In general, the order of importance of the three cost metrics was assumed to be fuel burn, empty weight, and then required engine power. Separate sizing exercises were performed for each of the three configurations. The results of steps 1 and 5 of the design process outlined in the Approach section are summarized here along with discussions of various design choices.

Compound Helicopter Sizing

The compound helicopter design for this study began with a single main rotor and tail rotor and a single pusher propeller mounted at the tail. This configuration is acceptable for smaller aircraft, but upon scaling up initial designs to meet the payload and range requirements, the large size of both the propeller and the anti-torque rotor caused them to interfere with each other. Multiple attempts were made at a configuration with the propeller at the tail, but they all required unreasonable rotor placements. Either the anti-torque rotor would need to be very far away from the centerline, or the propeller would need to be located very far aft. Both of these options would have unacceptable structural consequences, so the configuration was changed to include two propellers, with one mounted on each wing.

Lift share between the wing and the main rotor was varied with collective. The CAMRAD II twist optimization, described in the Rotor Optimization section of this paper, varied shaft angle to adjust lift share. This configuration would require a variable incidence hub, which would add

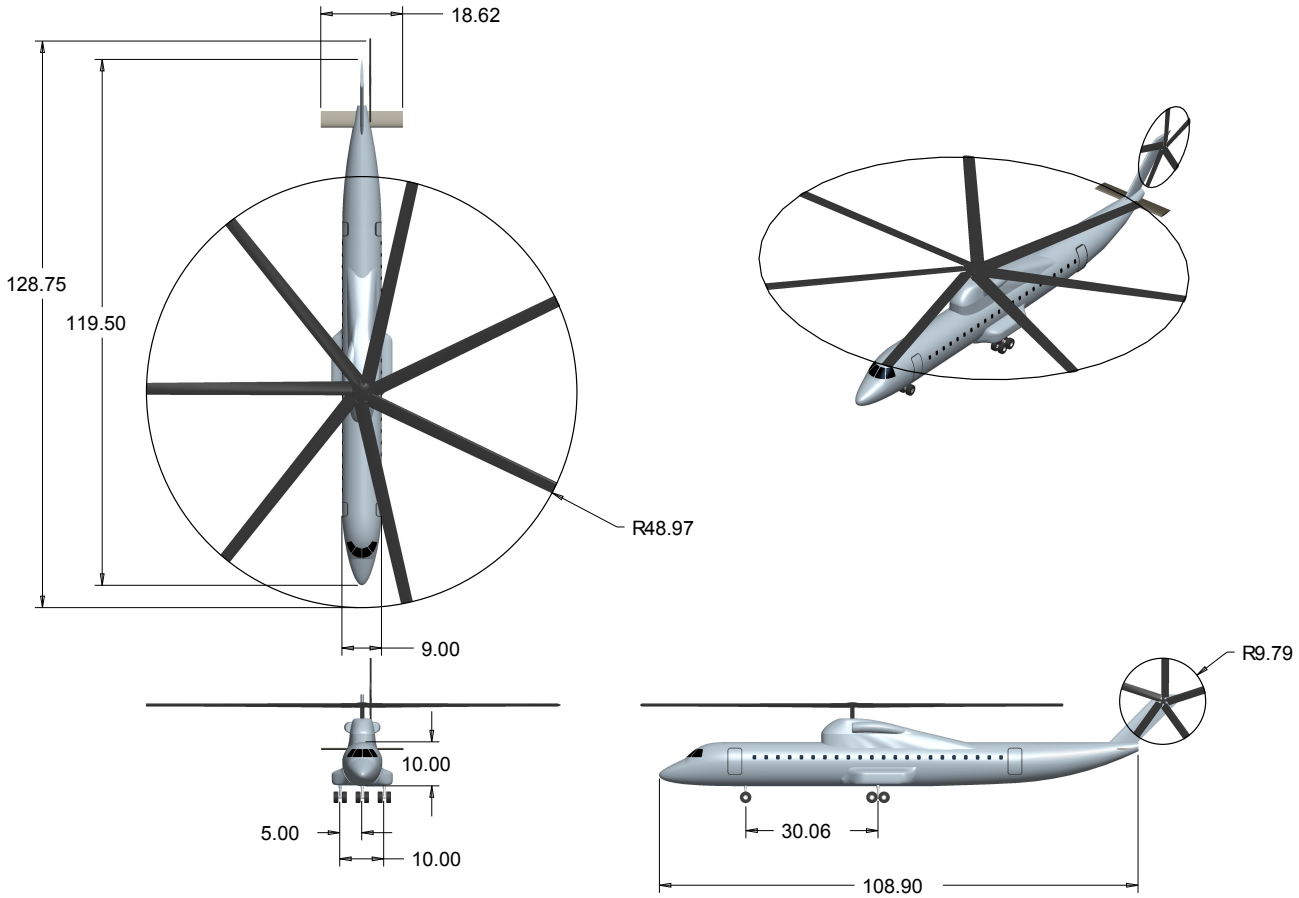

Figure 4. Illustration of the helicopter design

complexity and weight. If a variable incidence wing is required to minimize download in hover, the wing incidence could also be used to trim lift share. Collective was chosen as the simplest option, although it may not be realistically effective at very high advance ratios. Wing and hub incidence were fixed at 2 and 0 deg, respectively. The target lift share of the wing determined by the rotor optimization process was around 80%, and the final value used was 84.2% with the airframe level in cruise.

Design C_W/σ was fixed before sizing. For a large civil tiltrotor, Ref. 30 found that a C_W/σ of 0.151 is necessary for adequate maneuvering capability in low-speed flight. Since a compound helicopter is using both the main rotor and wings for lift in this condition, similar to a tiltrotor, C_W/σ was set equal to 0.151. While not a perfect solution, this should provide a good enough approximation to generate preliminary designs.

The number of main rotor blades was varied initially, but was ultimately set by practical limitations. Increasing the number of blades to 8 or even 9 yielded lighter and more efficient designs in NDARC, but these configurations would require very large hubs that border on or exceed realistic limitations. Large numbers of main rotor blades also result in very high aspect ratio blades that could present structural difficulties. For these reasons, a 7-bladed main rotor was chosen.

Main rotor tip speed in cruise was not optimized for this study, but was slowed to 450 ft/s to lower the rotor drag and reduce its required power. With design C_W/σ and tip speed set, the remaining major parameter that can be varied for the main rotor is disk loading. Figure 5 shows the results of sweeping main rotor disk loading. The two vertical axes are scaled differently to show the relative impact of disk loading on mission fuel and empty weight. In general, the disk loading has a larger relative impact on fuel weight than on empty weight. This result was observed for both the compound and the helicopter, which is presented later. The trends for engine power are very similar to those for fuel burn both before and after rotor twist optimization, so plots of engine power are omitted for brevity. The results suggest that a disk loading of either 12 or 14 lb/ft^2 would be the best choice, but these low disk loadings lead to exceedingly high blade aspect ratios of around 18 to 20. To obtain a reasonable blade aspect ratio while still maintaining relatively low empty weight and mission fuel, a disk loading of 15 lb/ft^2 was chosen, resulting in a blade aspect ratio of 17.3 – still high, but acceptable.

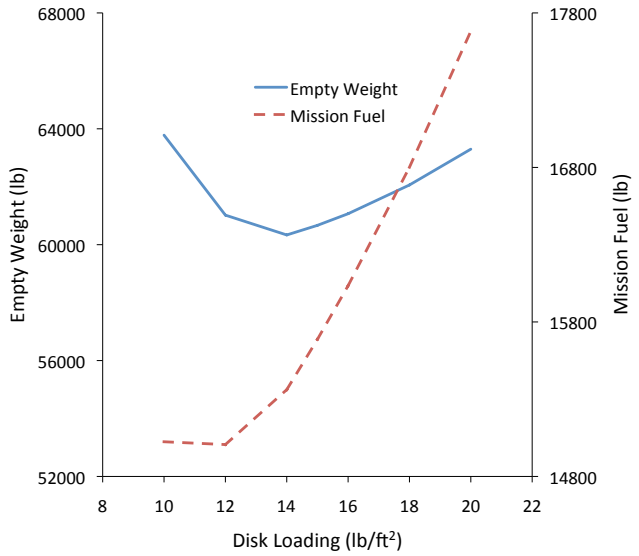

Figure 5. Compound helicopter empty weight and mission fuel as a function of disk loading

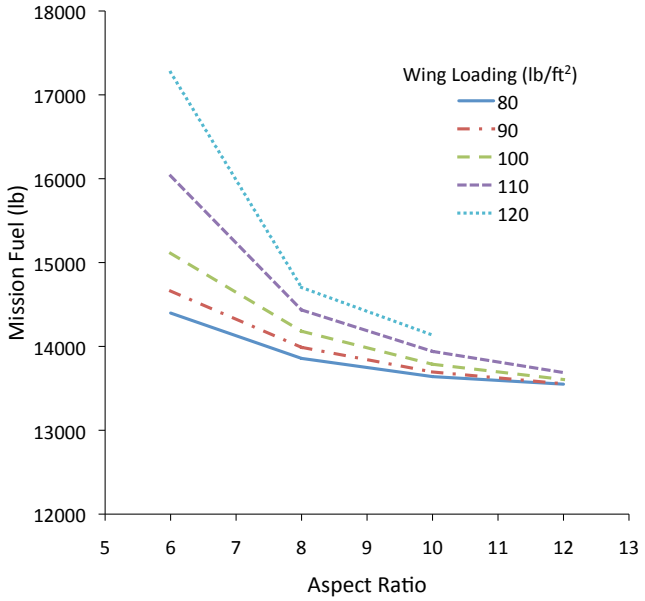

Figure 6. Compound helicopter mission fuel required as a function of wing loading and aspect ratio

With the disk loading chosen in addition to tip speed, C_W/σ, and number of blades, the main rotor is well-defined enough to move on to rotor blade optimization in CAMRAD II. That process is detailed in a later section.

Disk loading was also varied on the propellers, yielding an optimal radius. Again, a practical consideration was the determining factor. Since the propellers are located below the main rotor, they must be small enough to not interfere with it. This constraint resulted in a propeller radius of 7 ft.

The other major component to be optimized on the compound helicopter is the wing. The two parameters that were varied were the wing loading and the aspect ratio. Other parameters such as wing thickness, taper, and sweep were briefly studied, but showed little impact on the final designs. Span efficiency for the wing was assumed to be 0.8, which is a typical value for a turboprop aircraft. The effects of varying wing loading and aspect ratio are shown in Figs. 6 and 7.

From the results shown, it is clear that varying wing loading and aspect ratio has opposing effects on empty weight and mission fuel. The results for engine power closely resemble those for empty weight, so that plot is omitted. From an empty weight standpoint, the best design would have a low aspect ratio and low wing loading. For best fuel efficiency, high aspect ratio and low wing loading are optimal. As a compromise between empty weight and mission fuel, a wing loading of 100 lb/ft^2 and aspect ratio of 10 were chosen for the initial design.

After optimizing the rotor blades in CAMRAD II, wing loading, aspect ratio, and disk loading sweeps were run again to arrive at a final optimized design. The disk loading

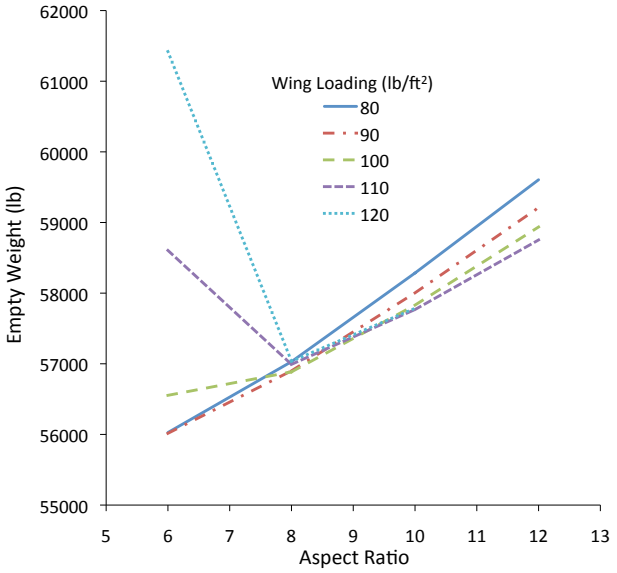

Figure 7. Compound helicopter empty weight as a function of wing loading and aspect ratio

results are shown in Fig. 8. These results show slightly different trends than the preliminary results in Fig. 5. Mission fuel weight still decreases with lower disk loading. Empty weight, however, continues to decrease as disk loading increases above 18 lb/ft^2, unlike in the preliminary results, where empty weight was minimized at a disk loading of 14 lb/ft^2. Again, a disk loading of 15 lb/ft^2 was chosen as a tradeoff between minimum fuel burn and minimum empty weight. Lower disk loadings would also have resulted in an unreasonably high blade aspect ratio.

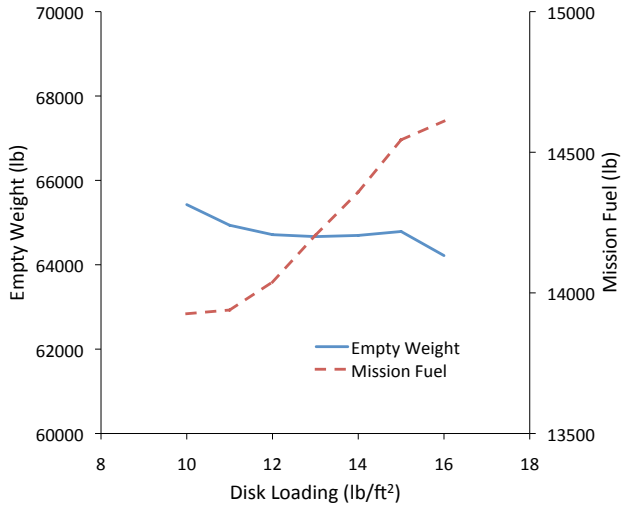

Figure 8. Compound helicopter empty weight and mission fuel as a function of disk loading – 2nd iteration

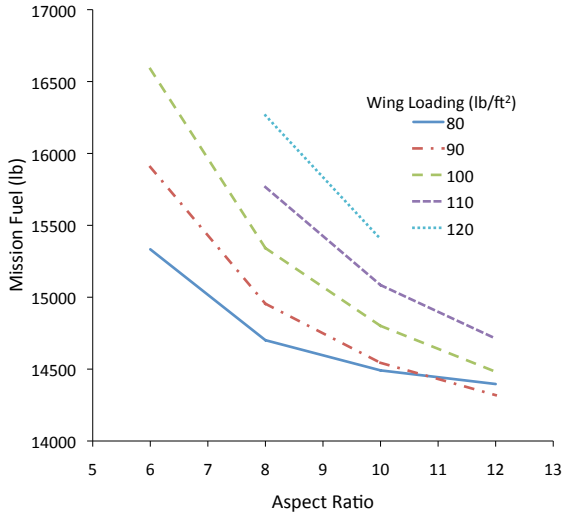

Figure 9. Compound helicopter mission fuel as a function of wing loading and aspect ratio – 2nd iteration

Results of the wing loading and aspect ratio sweeps using the optimized rotor are shown in Figs. 9, 10, and 11. The plots show similar trends to those generated before rotor optimization. Based on these results, a wing loading of 90 lb/ft^2 and an aspect ratio of 10 were chosen for the final design.

Tiltrotor Sizing

As a basis for comparison for the compound helicopter, two other designs were generated. The first was a 90-passenger tiltrotor. Many of the design parameters were left unchanged from their original LCTR2 values given in Ref. 29, including C_W/σ and hover rotor tip speed. These two parameters were set at 0.151 and 650 ft/s for maneuver and noise requirements, respectively—the same values as those used for the compound helicopter. Cruise rotor tip speed was set at 400 ft/s, reflecting the optimum found in Ref. 10.

The two parameters that were varied for the initial sizing of the tiltrotor were disk loading and wing loading. The results of these sweeps are shown in Figs. 12, 13, and 14. Note that the initial sweeps on the tiltrotor designs were performed with a design mission range of 1,000 nm.

Lowering the disk loading lowers the fuel burn and power required, but the empty weight starts to increase significantly at the lower disk loading values. This is primarily due to the high aspect ratio wings that are required to maintain separation between the larger rotors and the fuselage. Variations in wing loading did not have a very large effect on either fuel burn or engine power, but did significantly impact empty weight. Rotor clearance with the fuselage was again the main driver behind the empty weight, with increased wing loading decreasing the chord length and increasing the wing aspect ratio. The initial design used a wing loading of 105 lb/ft^2 and a disk loading of 14 lb/ft^2, which is slightly different than the wing loading of 107.4 lb/ft^2 and disk loading of 15.6 lb/ft^2 used for LCTR2.[29]

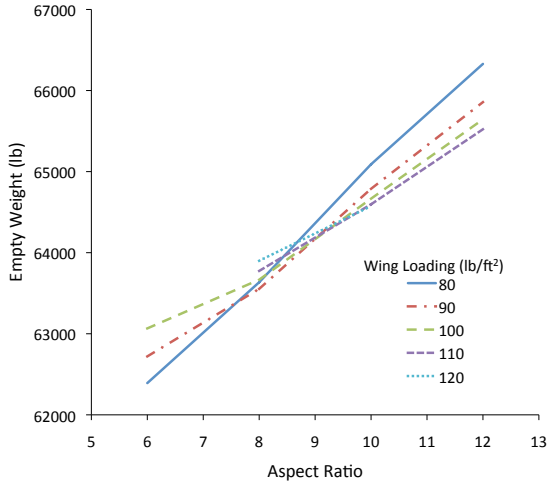

Figure 10. Compound helicopter empty weight as a function of wing loading and aspect ratio – 2nd iteration

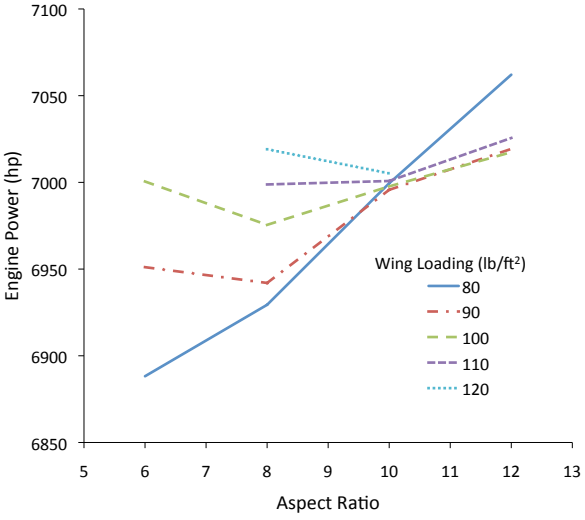

Figure 11. Compound helicopter power per engine as a function of wing loading and aspect ratio – 2nd iteration

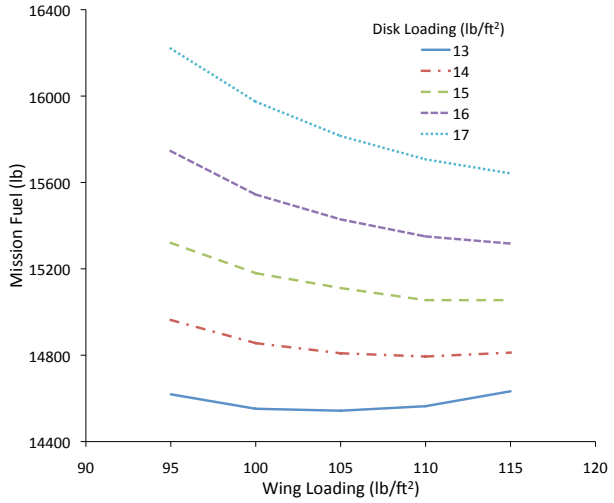

Figure 12. Tiltrotor fuel burn as a function of wing loading and disk loading – 1,000 nm range

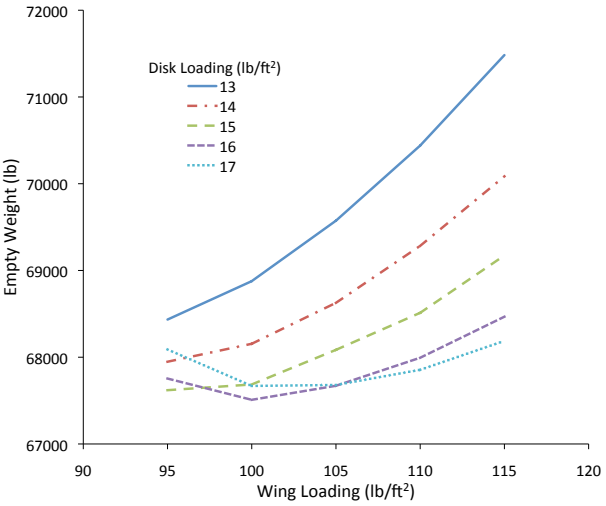

Figure 13. Tiltrotor empty weight as a function of wing loading and disk loading – 1,000 nm range

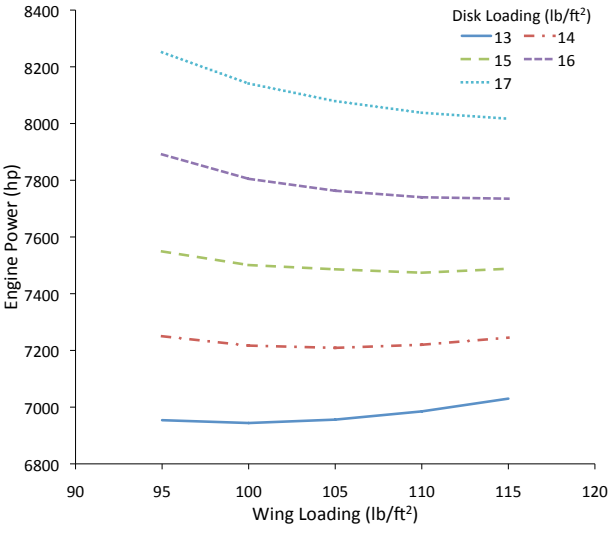

Figure 14. Tiltrotor power per engine as a function of wing loading and disk loading – 1,000 nm range

Rotor blade optimization was performed in CAMRAD II using the results of the initial sizing process. As was the case for the compound helicopter, wing loading and disk loading were again swept to arrive at a final design. The results of these sweeps for a design mission range of 500 nm are shown in Figs. 15, 16, and 17.

The designs with the optimized rotor and shorter design mission show different trends than those of the preliminary design. Also, the mission fuel for the 500 nm range tiltrotor is significantly more than half of the mission fuel for the 1,000 nm range design, indicating that the shorter range is not optimal for the tiltrotor. Despite the differences in the trends, the resulting optimal wing loading and disk loading are very close to their initial values. Wing loading remained unchanged at 105 lb/ft^2, while disk loading was increased to 15 lb/ft^2.

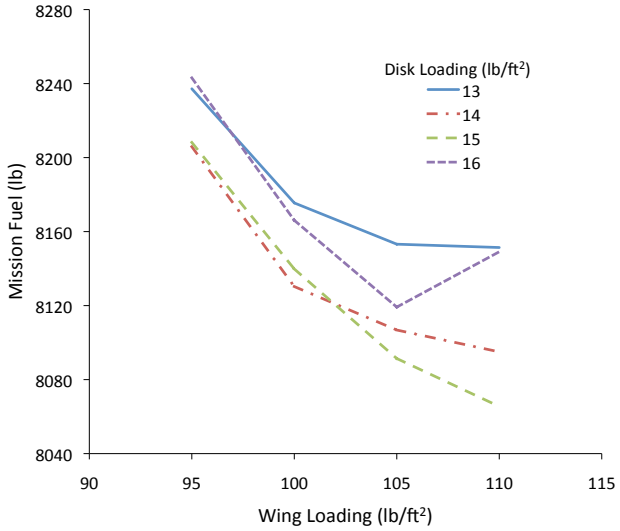

Figure 15. Tiltrotor fuel burn as a function of wing loading and disk loading – 2nd iteration, 500 nm range

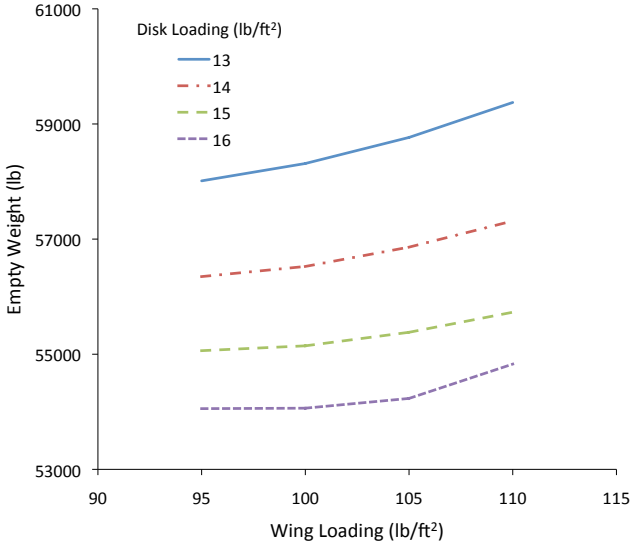

Figure 16. Tiltrotor empty weight as a function of wing loading and disk loading – 2nd iteration, 500 nm range

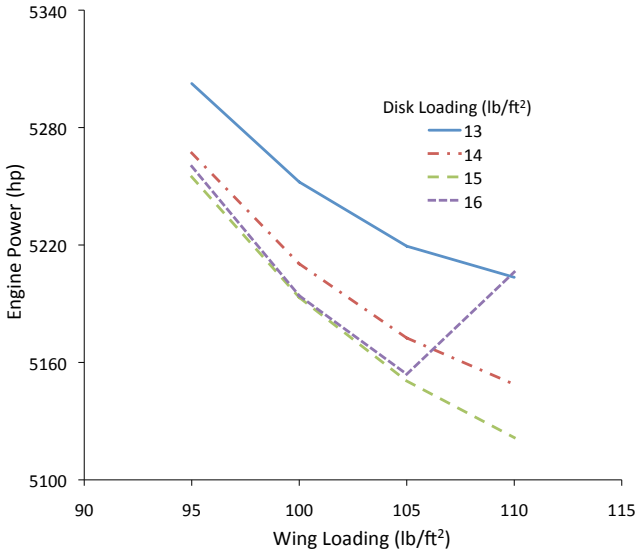

Figure 17. Tiltrotor engine power as a function of wing loading and disk loading – 2nd iteration, 500 nm range

Helicopter Sizing

The second basis for comparison for the compound helicopter was a conventional helicopter. The configuration is a scaled up version of a typical helicopter, and the initial performance model was based on a UH-60 rotor.

As was the case for the compound helicopter and the tiltrotor, the rotor tip speed for the helicopter was set at 650 ft/s to minimize noise. Design C_W/σ was set at a typical helicopter value of 0.09. The only parameter varied in the performance sweeps was disk loading. The results of the disk loading variations are shown in Fig. 18. Similar to the results for the compound helicopter, the engine power trends before and after rotor twist optimization closely followed those for fuel burn, so those results are omitted here.

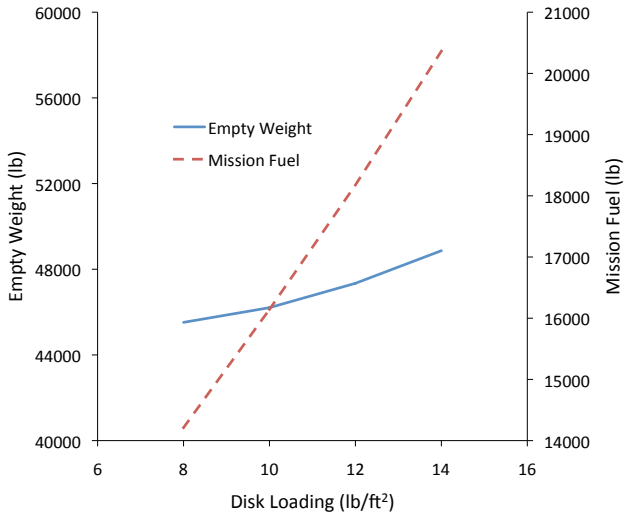

Figure 18. Helicopter empty weight and fuel burn as a function of disk loading

From Fig. 18, it appears that the best choice of disk loading would be 8 lb/ft^2 (or even lower), but the very low disk loading cases yielded rotors with unreasonably high blade aspect ratios and very large diameters. A value of 10 lb/ft^2 was chosen for the initial design.

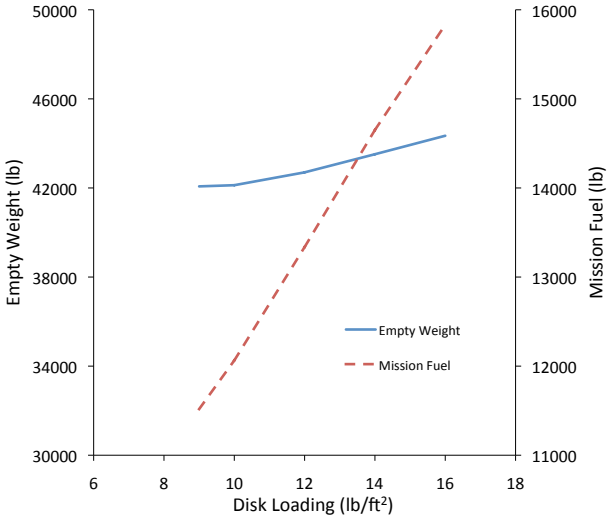

Figure 19. Helicopter empty weight and fuel burn as a function of disk loading – second iteration

After optimizing the main rotor, the trends of empty weight, fuel weight, and engine power closely resembled those found before rotor optimization. Empty weight and fuel burn results are shown in Fig. 19. Again, lowering disk loading had an effect of decreasing empty weight, fuel burn, and engine power required, but the blade aspect ratios and rotor diameters became unreasonably high. A disk loading of 10 lb/ft^2 was again chosen to obtain the best performance possible while keeping realistic physical constraints on the rotor.

ROTOR OPTIMIZATION

For each of the three designs, an optimization of the main rotor blade geometry (or both main rotors in the case of the tiltrotor) was performed after the first design iteration. CAMRAD II was used to analyze rotor performance given a rotor geometry and a set of flight conditions. The primary geometric variable for all three cases was blade twist. Blade taper (defined as the ratio of tip chord to root chord) was briefly examined, but the results suggested that taper ratios greater than 1 would provide the best performance. Since this result runs contrary to structural requirements, which were outside the scope of this study, ratios of 0.7 to 0.8 were used to reflect current design practices.

For all three rotorcraft configurations, a bilinear twist distribution with the transition point at 50% radius was used. Blade twist was swept around the expected optimum, and the actual optimum was generally bracketed in the first pass. The rotor diameter, solidity, and number of blades were determined by the initial sizing process detailed in the previous section. Two flight conditions were examined:

hover at takeoff conditions and cruise at V_{br}. These flight conditions set the atmospheric properties, speed, and generally C_T/σ.

CAMRAD II was used to analyze the performance of the rotors. For all three configurations, an isolated rotor was modeled, with no interference effects from wings or fuselage. Previous studies have shown that the change in rotor power due to rotor-wing interference for both compound helicopters and tiltrotors is small enough to neglect for a conceptual design study such as this, although for a tiltrotor, rotor interference on the wing is important.[12,29]

After running the various blade twist cases, Pareto fronts were generated showing the tradeoffs between hover and cruise performance. For a handful of cases on the Pareto front, the induced power factor κ and the mean blade drag coefficient $c_{d\ mean}$ were input into NDARC and the aircraft were resized. The optimum twist was then chosen based on which combination of κ and $c_{d\ mean}$ resulted in the lightest, most efficient aircraft. The following sections detail the results of the twist optimization process for the compound helicopter, tiltrotor, and helicopter. This section covers steps 2-4 in the design process outlined in the Approach section of this paper.

Compound Helicopter Rotor Optimization

The twist rate on the compound helicopter main rotor was swept from –3 to 6 deg/R (R here is the rotor radius) on the inboard section and –18 to 0 deg/R on the outboard section. Hover efficiency was represented by rotor figure of merit, while cruise efficiency was represented by the combined rotor-wing effective lift-to-drag ratio. Effective drag for cruise performance was calculated using the equation shown below:

$$D_{eff} = \frac{1}{\eta_{prop}}\left(D_{wing} + D_{rotor}\right) + \frac{P_{rotor}}{V}$$

In the above equation η_{prop} is the propulsive efficiency of the compound helicopter's propellers, in this case 0.84. Rotor drag and power, D_{rotor} and P_{rotor}, respectively, are output directly by CAMRAD II, and velocity V is specified by the cruise condition. Wing drag, D_{wing}, was calculated as the sum of induced and parasite drag using the standard wing drag equation:

$$D_{wing} = qS\left(C_{D_o} + \frac{1}{\pi ARe}\left(\frac{L_{wing}}{qS}\right)^2\right)$$

q, S, AR, and e are the dynamic pressure, wing planform area, wing aspect ratio, and span efficiency, respectively. The parasite drag coefficient C_{D_o} was assumed to be 0.008. L_{wing}, the wing lift, was determined by subtracting the rotor lift, calculated by CAMRAD II, from the total lift required.

In the case of the compound helicopter, unlike the helicopter and tiltrotor, the rotor lift was not specified as an input to CAMRAD II. This is because the lift share between the wing and main rotor still needed to be determined. Rotor shaft angle and collective were varied to obtain results for various thrust levels. L/D_{eff} was then computed based on CAMRAD II outputs using the above equations. The maximum L/D_{eff} was found at a collective of 0 and shaft angle of 4 degrees, resulting in the wing carrying 76-85% of the total lift, depending on twist. The results of the twist sweep for a collective of 0 and shaft angle of 4 degrees are shown in Fig. 20.

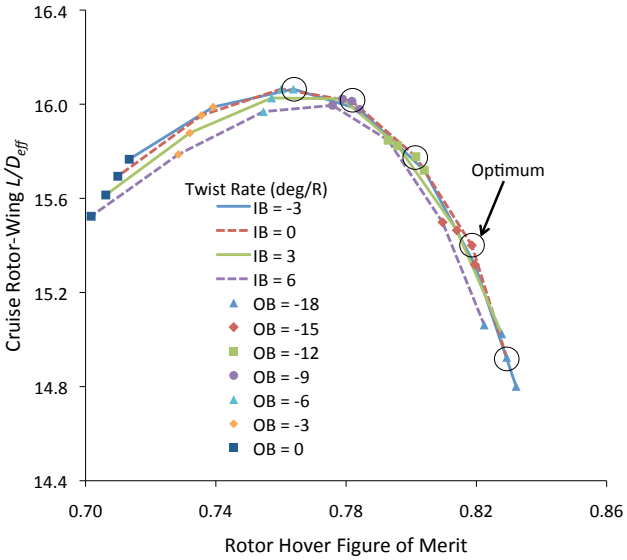

Figure 20. Effects of twist variation on compound helicopter hover figure of merit and cruise rotor-wing L/D_{eff}

The circles in Fig. 20 indicate the five twist distributions on the Pareto front that were tested in NDARC to find the optimum. As shown, the best choices for inboard and outboard twist rates were 0 and –15 deg/R, respectively. For the compound helicopter, hover figure of merit showed higher variation with changes in twist than did effective lift-to-drag ratio. This result, in addition to the fairly short range of the design mission, led to hover performance having greater influence than cruise performance on the final selection of rotor blade twist.

To create the NDARC rotor performance model for the compound helicopter in hover, C_T/σ was swept across a range of values. For cruise, several speed sweeps were run with C_T/σ held at different values.

Tiltrotor Rotor Optimization

For the tiltrotor design, the twist rates were swept from –54 to –40 deg/R inboard and –28 to –38 deg/R outboard. Hover efficiency was represented by hover figure of merit, and cruise efficiency was represented by the propulsive efficiency of the rotors in axial forward flight. Hover and cruise thrust conditions were calculated as fallout from the sizing process. CAMRAD II results for the rotor twist variations for the tiltrotor design are shown in Fig. 21.

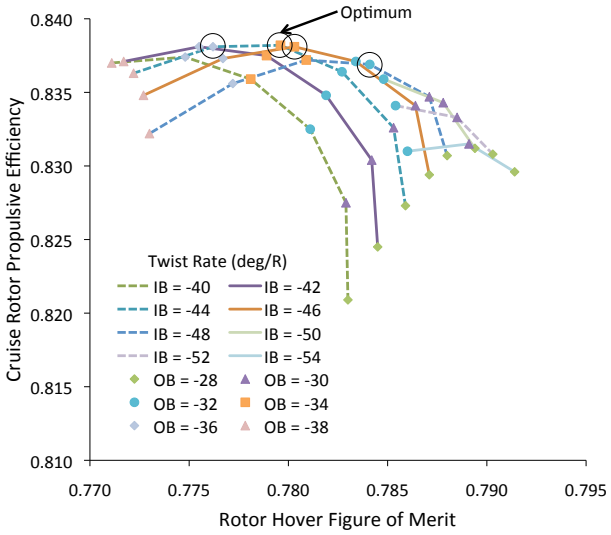

Figure 21. Effects of twist variation on tiltrotor hover figure of merit and cruise propulsive efficiency

The optimal twist for the tiltrotor was found to be –44 deg/R inboard and –34 deg/R outboard. For this design, cruise performance had the greatest influence on the selection of blade twist. While hover figure of merit varied more strongly with twist than did propulsive efficiency, the twist distribution for the tiltrotor was selected based on a design mission of 1,000 nm. This resulted in a rotor design that was heavily dominated by cruise performance.

The tiltrotor hover performance model was determined by sweeping C_T/σ. For cruise performance, both speed and angle of attack were swept at different values of X/q, the rotor force in the wind axis normalized by dynamic pressure.

Helicopter Rotor Optimization

The range of blade twist values tested for the helicopter design was –12 to –3 deg/R inboard and –18 to –10 deg/R outboard. Hover figure of merit was the primary indicator of hover performance, while rotor L/D was used for cruise.

Again, the values for C_T/σ and forward thrust were determined in the sizing process using NDARC. The resulting performance curves are shown in Fig. 22.

For the helicopter design, the optimal twist was –9 deg/R inboard and –16 deg/R outboard. Like the compound helicopter design, the conventional helicopter rotor showed more variation in hover performance than in cruise performance with changes in twist. Accordingly, the hover performance had a greater impact on the final selection of blade twist.

The helicopter rotor performance model for hover was determined in the same manner as that for the compound helicopter and the tiltrotor, by sweeping C_T/σ. For cruise, speed was swept for a few values of C_T/σ and a set X/q.

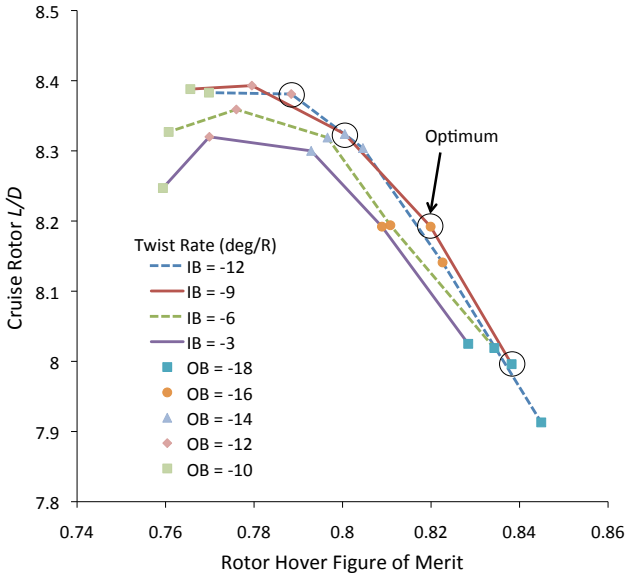

Figure 22. Effects of twist variation on helicopter hover figure of merit and rotor L/D in cruise

PERFORMANCE ANALYSIS

A summary of the key design and performance parameters for the compound helicopter, tiltrotor, and helicopter designed to a 500 nm range are contained in Table 3.

The first four rows of Table 5 are NDARC outputs from the sizing process and are reproduced from Table 2. These values represent the traditional drivers of aircraft purchase and operating cost. Production of CO_2 is based on a typical value of 3.16 pounds of carbon dioxide per pound of jet fuel burned.[31] In future scenarios where CO_2 production may be regulated under the European Union's Emissions Trading Scheme or another cap and trade type of policy, emissions could become a cost driver as well.

Table 3. Major design and performance parameters of the three final designs

	Compound	Tiltrotor	Helicopter
Empty Weight (lb)	64,789	55,380	42,060
Max TO Wt. (lb)	115,665	97,449	86,617
Engine Power (HP per engine)	6,996	5,150	4,020
Fuel Burn (lb)	14,545	8,098	11,999
CO_2 Produced (lb)	45,962	25,590	37,917

The results suggest that the compound helicopter design would have the highest airframe purchase and operating costs compared with the conventional helicopter and tiltrotor, due to its high weight and fuel burn. The helicopter is relatively limited, however, in both maximum speed and altitude, so it may not be a better choice from an operations standpoint. The tiltrotor design would likely have the lowest operating costs, with the lowest fuel burn, while the

helicopter has the lowest empty weight, indicating the lowest airframe cost. Additionally, the conventional helicopter is a simpler and more thoroughly understood design than a tiltrotor or a compound helicopter, which would likely push its airframe cost even lower.

Once the final designs were generated, various parameter sweeps were completed to determine the performance of the three designs under various operating conditions. Payload-range curves are shown in Fig. 23.

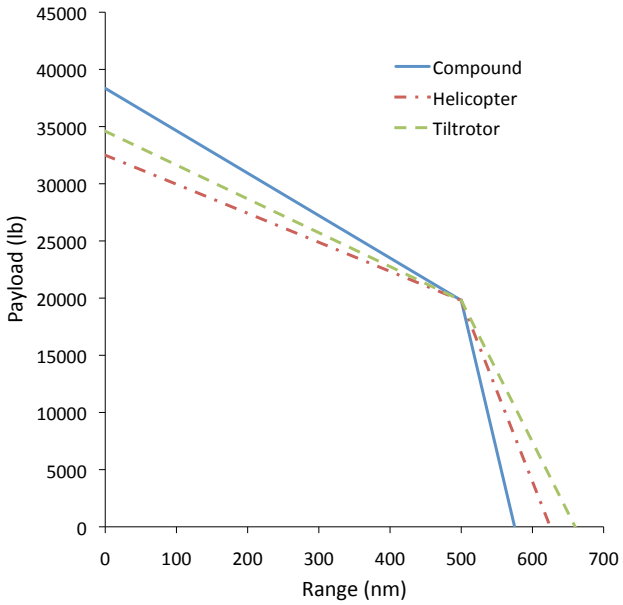

Figure 23. Payload-range diagram for three final designs

The calculation of maximum payload at zero range eliminates the climb and cruise segments of the design mission, but leaves the taxi and reserve segments described in Table 1. The reserve segments for zero range are flown at 5,000 ft altitude. Maximum range at zero payload is the primary mission distance, while maintaining the reserve mission segments. Of the three designs, the compound helicopter has the highest fuel weight fraction for the design mission, giving it the highest useful load capacity, so it can carry the heaviest payload at zero range. The tiltrotor has the farthest range at zero payload, due to its higher cruise efficiency and lower weight.

Plots showing variation with altitude of speed for maximum range and endurance along with maximum speed are presented in Figs. 24, 25, and 26. All three curves are calculated at design gross weight, and maximum speed is calculated at maximum continuous power. The intersection of the curves for maximum endurance and maximum speed shows the overall maximum altitude for each design. The altitude and approximate speed each aircraft flies in the cruise segment of the design mission is indicated as well. The actual speed flown in the design mission is slightly different than the speed indicated, because the aircraft weight in cruise is less than design gross weight. The three plots are scaled equally for the sake of comparison.

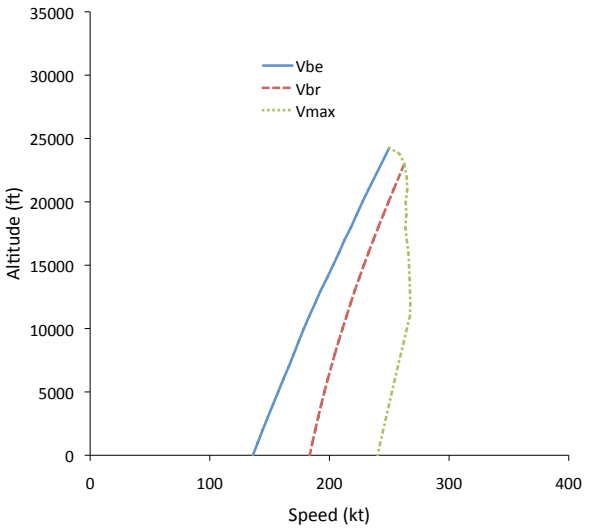

Figure 24. Compound helicopter maximum effort speeds

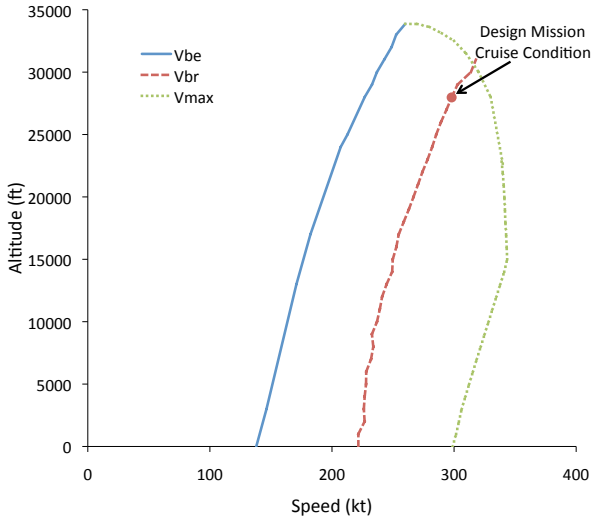

Figure 25. Tiltrotor maximum effort speeds

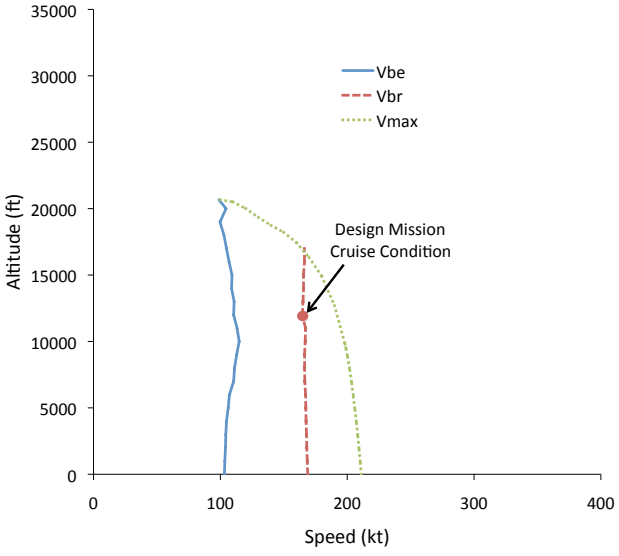

Figure 26. Helicopter maximum effort speeds

Of the three designs, the tiltrotor has the largest operating envelope, with both the highest maximum speed and highest maximum altitude. The helicopter has the smallest, and the compound helicopter falls in between.

DISCUSSION AND CONCLUSIONS

The purpose of this study was to generate a design for a large civil compound helicopter capable of carrying 90 passengers and compare its performance against a similarly sized tiltrotor and conventional helicopter. The design mission was intended to be shorter than optimal for a tiltrotor and longer than optimal for a conventional helicopter. Sizing of the three designs was carried out in NDARC, and rotor performance models were generated using CAMRAD II. The performance of all three designs was further evaluated to determine their respective envelope of operations.

While this study did not show the compound helicopter to be a competitive design for the civil mission described, there are several possibilities for design changes that could drive down its weight and fuel burn. This research focused on a single design mission with a 500 nm cruise segment, which may not be optimal for the compound helicopter design presented here. Further investigations may reveal a different design mission that is better suited to this aircraft.

For this study, the design included an anti-torque tail rotor, which would not be necessary if the propellers on the wings can be used for anti-torque in hover. This configuration is used for both the Eurocopter X3 and in Ref. 11 and could provide significant weight savings, but compromises in propeller efficiency and placement on the wing could drive up both weight and fuel burn. There are multiple other compound helicopter configurations not analyzed for this study that could have lower costs as well.

The compound helicopter designed for this study assumed a faired hub, but did not use very aggressive application of drag reduction technology. The cumulative drag on the hubs of the main and tail rotors accounted for approximately 40 percent of total aircraft drag in cruise, so it was a very large driver of fuel burn. Additional drag reduction could be accomplished by improving the wing span efficiency, but any such technology improvements in the future would presumably also be available for tiltrotor designs. A more rigorous optimization of wing lift share would likely improve performance as well.

Environmental considerations may also drive future rotorcraft designs, but it is uncertain what the impact would be. If CO_2 emissions are the metric used, fuel burn will become even more important, but if metrics that track multiple pollutants are used, determining the optimal design may not be so simple. More complex environmental metrics depend on variables such as altitude and engine throttle setting and can drive aircraft designs away from minimum weight and fuel burn.[32]

This study provided a starting point for the design of a large civil compound helicopter. The results presented suggest that this type of design would have higher cost than either a similarly sized conventional helicopter or tiltrotor. Several possible options for reducing the compound helicopter cost to competitive levels have been suggested and will be the subject of future research.

ACKNOWLEDGEMENTS

The authors would like to thank Alexander Amy and Eduardo Solis of NASA Ames Research Center for preparing the aircraft drawings and Dr. Hyeonsoo Yeo for his assistance in generating the CAMRAD II rotor models.

REFERENCES

1. Couluris, G., C. Hange, D. Wardwell, D. Signor, and J. Phillips, "A Potential Impact Analysis of ESTOL Aircraft on Newark Airport Operations," American Institute of Aeronautics and Astronautics Modeling and Simulation Technologies Conference and Exhibit, Hilton Head, SC, August 20-23, 2007.

2. Chung, W., D. Linse, A. Paris, D. Salvano, T. Trept, T. Wood, H. Gao, D. Miller, K. Wright, R. Young, V. Cheng, "Modeling High-Speed Civil Tiltrotor Transports in the Next Generation Airspace," NASA/CR-2011-215960, October 2011.

3. Johnson, W., G. Yamauchi, and M. Watts, "NASA Heavy Lift Rotorcraft Systems Investigation," NASA TP-2005-213467, December 2005.

4. Taylor, J., *Jane's All the World's Aircraft, 1969-70*. London: Jane's Yearbooks, 1969.

5. Eurocopter, *The X3 Concept* (Video), http://www.eurocopter.com/site/en/ref/Videos_1101.html, accessed December 14, 2011.

6. Eurocopter, "The Eurocopter X3 Hybrid Helicopter Exceeds its Speed Challenge," Eurocopter Press Release, Marignane, France, May 16, 2011.

7. NAVAIR, "V-22 Osprey 2010 Guidebook," NAVAIR PMA-275, CN 10-28, 2010.

8. Frawley, G., *The International Directory of Military Aircraft*, p. 148. Aerospace Publications Pty Ltd., 2002.

9. Jackson, P., *Jane's All the World's Aircraft, 2003-2004*. London: Jane's Yearbooks, 2003.

10. Acree, C.W. Jr., H. Yeo, and J. Sinsay, "Performance Optimization of the NASA Large Civil Tiltrotor," International Powered Lift Conference, London, UK, July 22-24, 2008.

11. Yeo, H. and W. Johnson, "Optimum Design of a Compound Helicopter," *Journal of Aircraft*, Vol. 46, No. 4, July-August 2009.

12. Moodie, A. and H. Yeo, "Design of a Cruise Efficient Compound Helicopter," American Helicopter Society 67th Annual Forum, Virginia Beach, VA, May 3-5, 2011.

13. Silva, C., H. Yeo, and W. Johnson, "Design of a Slowed-Rotor Compound Helicopter for Future Joint Service Missions," American Helicopter Society Aeromechanics Specialists' Conference, San Francisco, CA, January 20-22, 2010.

14. Kottapalli, A. and F. Harris, "Converting a C-130 Hercules into a Compound Helicopter: A Conceptual Design Study," AHS Aeromechanics Specialists' Conference, San Francisco, CA, January 20-22, 2010.

15. Johnson, W. "NDARC. NASA Design and Analysis of Rotorcraft." NASA TP 2009-215402, December 2009.

16. Johnson, W. "NDARC — NASA Design and Analysis of Rotorcraft. Theoretical Basis and Architecture." American Helicopter Society Specialists' Conference on Aeromechanics, San Francisco, CA, January 2010.

17. Johnson, W. "NDARC — NASA Design and Analysis of Rotorcraft. Validation and Demonstration." American Helicopter Society Specialists' Conference on Aeromechanics, San Francisco, CA, January 2010.

18. Johnson, W., "Technology Drivers in the Development of CAMRAD II," American Helicopter Society Aeromechanics Specialist Meeting, San Francisco, California, January 1994.

19. Johnson, W. "Rotorcraft Aeromechanics Applications of a Comprehensive Analysis." HeliJapan 1998: AHS International Meeting on Rotorcraft Technology and Disaster Relief, Gifu, Japan, April 1998.

20. Johnson, W. "Rotorcraft Aerodynamic Models for a Comprehensive Analysis." American Helicopter Society 54th Annual Forum, Washington, D.C., May 1998.

21. Johnson, W. "Calculation of Tilt Rotor Aeroacoustic Model (TRAM DNW) Performance, Airloads, and Structural Loads." American Helicopter Society Aeromechanics Specialists' Meeting, Atlanta, GA, November 2000.

22. Yeo, H. "Calculation of Rotor Performance and Loads Under Stalled Conditions." American Helicopter Society 59th Annual Forum, Phoenix, AZ, May 2003.

23. Yeo, H., Bousman,W. G., and Johnson,W., "Performance Analysis of a Utility Helicopter with Standard and Advanced Rotor," *Journal of the American Helicopter Society*, Vol. 49, No. 3, July 2004.

24. Yeo, H., and Johnson, W., "Assessment of Comprehensive Analysis Calculation of Airloads on Helicopter Rotors," *Journal of Aircraft*, Vol. 42, No. 5, Sept.–Oct. 2005.

25. Yeo, H., and Johnson, W., "Prediction of Rotor Structural Loads with Comprehensive Analysis," *Journal of the American Helicopter Society*, Vol. 53, No. 2, April 2008.

26. Harris, F.D. "Rotor Performance at High Advance Ratio; Theory versus Test." NASA CR 2008-215370, October 2008.

27. Hess, R.W. and H.P. Romanoff, "Aircraft Airframe Cost Estimating Relationships," The RAND Corporation, Santa Monica, CA, December 1987, R-3255-AF.

28. Morrison, J., P. Bonnefoy, R. J. Hansman, and S. Sgouridis, "Investigation of the Impacts of Effective Fuel Cost Increase on the US Air Transportation Network and Fleet," 10th AIAA Aviation Technology, Integration, and Operations (ATIO) Conference, Fort Worth, TX, September 13-15, 2010.

29. Acree, C. W., Jr., "Integration of Rotor Aerodynamic Optimization with the Conceptual Design of a Large Civil Tiltrotor," American Helicopter Society Aeromechanics Conference, San Francisco, CA, January 20-22, 2010.

30. Yeo, H., J. Sinsay, and C. W. Acree, Jr., "Selection of Rotor Solidity for Heavy Lift Tiltrotor Design," *Journal of the American Helicopter Society*, Vol. 55, No. 1, January 2010.

31. Intergovernmental Panel on Climate Change, Aviation and the Global Atmosphere, Cambridge Univ. Press, Cambridge, England, U.K., 1999.

32. Schwartz, E. and I. Kroo, "Aircraft Design: Trading Cost and Climate Impact," 47th AIAA Aerospace Sciences Meeting, Orlando, FL, January 5-8, 2009.